International Journal of Geology, Earth & Environmental Sciences ISSN: 2277-2081 (Online)
An Open Access, Online International Journal Available at http://www.cibtech.org/jgee.htm
2014 Vol. 4 (1) January-April, pp. 28-36/Karl et al.
Research Article

HETEROGENEITY OF AN OIL SPILL

[*]Karl H. Szekielda[1], Karen W. Patterson[2], Jeffrey H. Bowles[2] and Michael R. Corson[2]
[1]Hunter College, City University of New York, 695 Park Avenue, New York, NY 10065
[2]Naval Research Laboratory, 4555 Overlook Ave., SW, Washington, DC 20375
[*]Author for Correspondence

ABSTRACT
Data from the Hyperspectral Imager for the Coastal Ocean (HICO) were used to investigate distribution characteristics of the 2010 oil spill in the Gulf of Mexico. Strong reflectance in the near infrared was observed over patches of oil and at wavelengths below 0.5 µm, absorption was observed without the presence of major absorption bands. The HICO image revealed the heterogeneity in the distribution of oil and showed that dispersal and accumulation of oil may appear in streaks that vary in width and length. This distribution pattern in the form of streaks is most probably caused through formation of wind rows and as a result of accumulation in the convergence zone of internal waves.

Keywords*: Gulf of Mexico Oil Spill, Hyperspectral Remote Sensing, HICO*

INTRODUCTION
Oil spills that occurred during the last decades are responsible for changes and damages of the coastal environment and once they reach the coast, affect many economies and in particular those that are based on fishery and tourism. The largest offshore spill in US history in the Gulf of Mexico on April 20, 2010resulted from the Deepwater Horizon drilling rig explosion and had an estimated flow at 35,000 to 60,000 barrels of crude oil per day and totaled until the spill source was capped 4.9 million barrels. The resulting spill quickly spread and it was shown that the effects of wave-induced drift and dispersion led to a spill displacement of around 30 km in about five days (Pugliese *et al.*, 2011).
Oil spills contain many toxic substances including polycyclic aromatic hydrocarbons that may enter through the food chain to marine mammals, fish, and aquatic invertebrates. Problematic is the long-term effect of bioaccumulation of toxic matter in oil spills, even at low concentrations, that can start in surface water through uptake by phytoplankton, and aggregation of surface floating macroalgae (Gower *et al.*, 2006) that can be coated very quickly with oil and can become immediately stressed (Johnson and Richardson, 1977).
Oil on a calm water surface may appear as silvery sheen, rainbow sheen, reddish brown or dark (Jha *et al.*, 2008), but water-leaving radiance also depends on the oil type and its thickness (Howari, 2004). Carnesecchi *et al.*, (2008) modeled the spectral behavior of oil at water surfaces and took into consideration the refractive index, which is higher than that of water, and its absorption coefficient, which is stronger than that of water. In addition, the signature of oil on water is affected by the optical properties of the water column itself and sea state as well as by the incident light distribution.
Factors which affect the ability of an oil spill to spread at the sea surface include surface tension, specific gravity and viscosity, but oil spills don't build a homogenous layer because they disperse and migrate, and due to chemical breakdown, change their physical and chemical properties (Thiel and Gutow, 2005). Wave and wind action further accelerates the dispersion of oil, and oxidation may produce water-soluble compounds. Evaporation of the low molecular fraction of oil contributes to the weathering of spilled oil and a large portion of the volatile components of an oil spill may evaporate within one day of the spill (Fingas, 1996) while the remaining heavy part of weathered oil can persist for a long period of time.
The uneven distribution of spilled oil at the sea surface can be demonstrated with a MODIS image at 500 m resolution which is shown in Figure 1. Although fine-scale features in the oil slick are not recognized at this resolution, it is evident that spectral modification appears during the dispersal of oil with an indication that the patchiness of the oil spill changes during its spreading and transport away from the spill source.

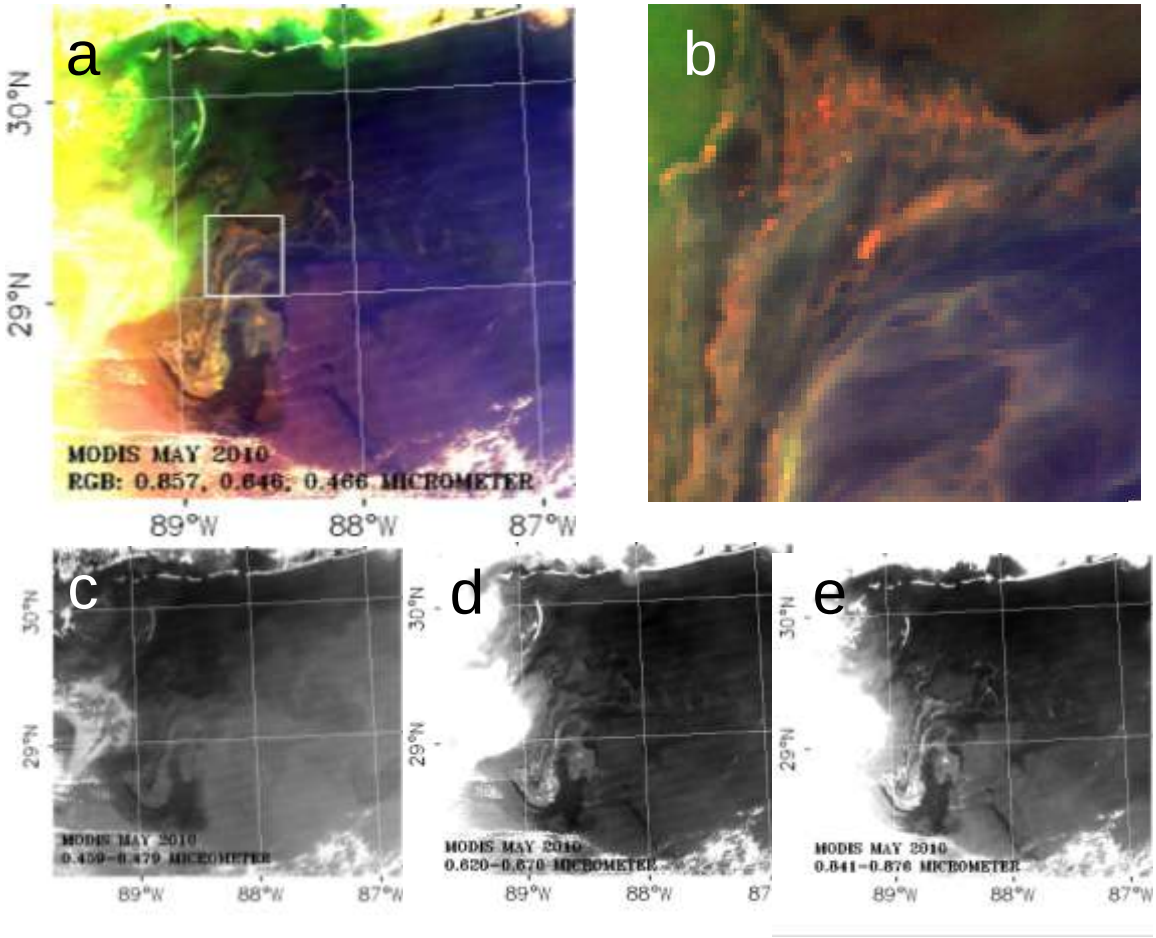

Figure 1: MODIS reflectance acquired on May 24, 2010 at 500 meter resolution. 1a: Color composite RGB based on the central wavelengths 0.857 µm, 0.648 µm, and 0.466 µm, respectively. 1b: Enlargement of the square shown in 1a. Figures 1c through 1e are the different channels used for the color composites in *a* and *b*.

At the beginning of the Deep Horizon oil spill, concern was expressed about the possibility that oil would enter the Loop Current and be further transported into the Gulf Stream system.
However, Liu *et al.*, (2011) found that the main body of the surface oil slick remained around the well site and on the Northern Gulf shelf, and only a small amount of the surface oil was entrained into the northern part of the Loop Current system in mid-May 2010.
This is also confirmed with the surface circulation that was charted during the time of HICO data acquisition and is shown in Figure 2 with the formation of an anticyclonic eddy that was in progress but separated from the northern part of the Loop Current in the latter part of May 2010 (Liu *et al.*, 2011). However, the prevailing winds played the major role in pressuring the oil towards the coasts along the northern Gulf and parallel to the Loop Current's development that blocked the oil spill to the Florida Strait (Le-Hénaff *et al.*, 2012).

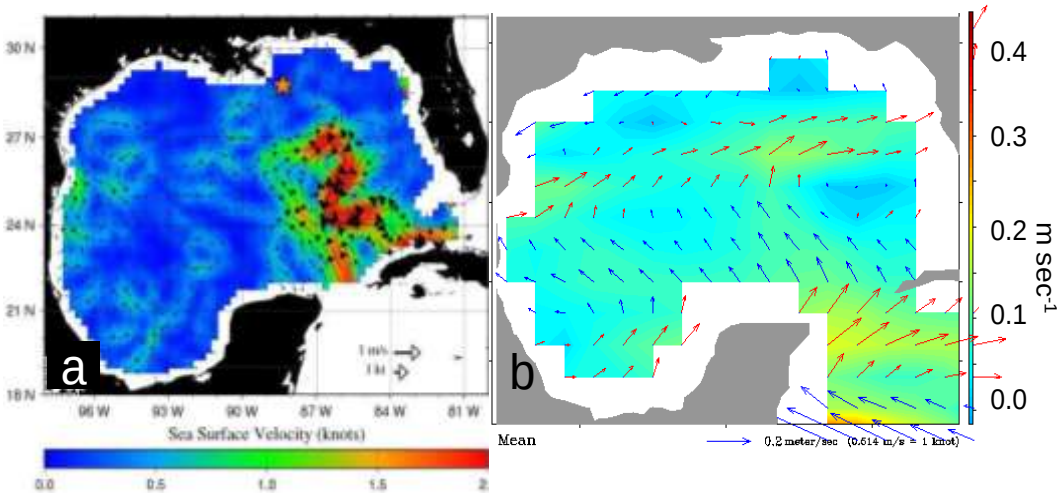

Figure 2a: Surface currents estimated by real-time meso scale radar altimetry on May 23, 2010 (NASA/JPL University of Colorado). 2b: Five-day interval surface currents (m sec^{-1})on May 22, 2010. The current field is resolved at one degree square and is based on analysis with OSCAR-NOAA.

Monitoring of oil spills has been successfully accomplished with several remote sensing systems that are available (Brekke and Solberg, 2005) and have been reviewed by Klemas (2010). Sensors include those that operate in the passive mode such as infrared cameras, optical sensors, infrared/ultraviolet systems, and microwave radiometers, whereas active sensors include radar and laser systems. In the visible, oil at the air-sea interface has intrinsic properties and its spectral signatures can best be resolved with hyperspectral instruments (Andreoli *et al.,* 2007). A detailed summary was provided by Leifer *et al.,* (2012) on the state of the art in satellite and airborne remote sensing of marine oil spills with specific application to the BP Deepwater Horizon oil spill. The problem with slick identification is that not a single sensor covers the requirements for identifying the characteristics of an oil spill. SAR, for instance, provides signals that may identify falsely and does not allow discrimination between natural and anthropogenic slicks.

In this study the analysis of one image is used from the Hyperspectral Imager for the Coastal Ocean (HICO) with the aim to define the surface pattern of oil-covered water that resulted from the spill in the Gulf of Mexico. HICO is not an operational scanner system, rather it is the first space-borne hyperspectral sensor designed specifically for the coastal ocean and estuarine waters and other shallow-water areas and operates within a spectral range of about 0.40 to 0.90 µm. The sensor is installed on the International Space Station (ISS) and records a cross-track and along-track FOVs of 42 km (at nadir) and 192 km, respectively. Details on the sensor design and its performance have been documented by Corson *et al.*, (2010), Lucke *et al.*, (2010) and Lucke *et al.*, (2011). The advantage of HICO is its high-signal-to-noise ratio and a further improvement, compared to other ocean color observing satellite systems, is the ground resolution of about 100 m.

RESULTS AND DISCUSSION

Results

The image analyzed is shown as a color composite image in Figure 3 and shows partial cloud contamination in the north-west, displayed in white, and the Mississippi effluent is displayed in green. The southern part of the image shows clear Gulf water and is presented in magenta whereas the oil spill is

recognized as light purple and reveals streak-like distribution of surface oil. The image does not completely cover the whole oil spill area as can be seen with the position of the former oil rig in Figure 3.

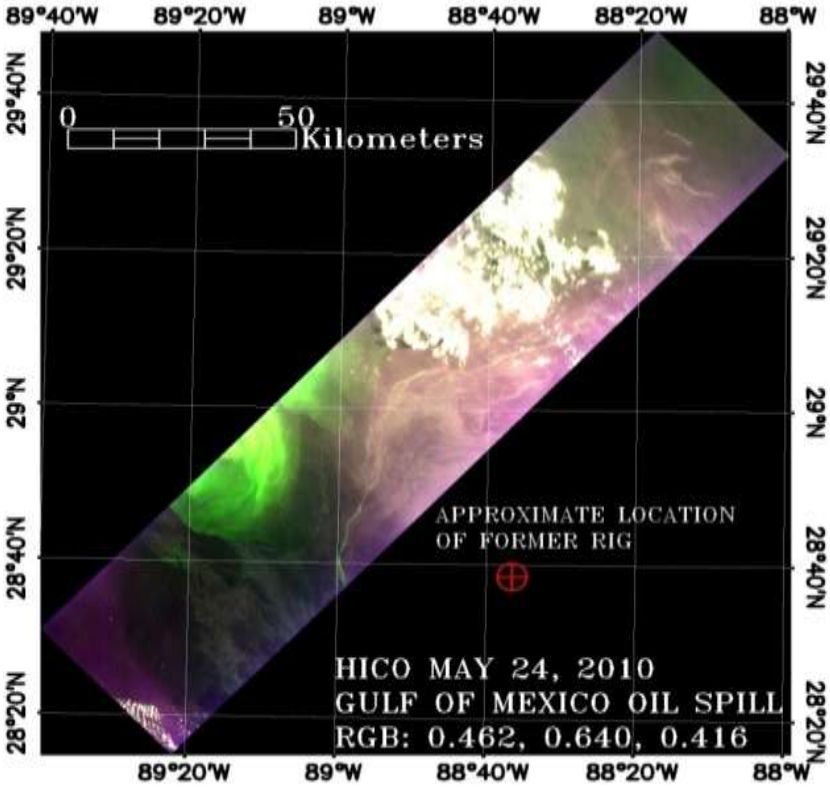

Figure 3: RGB for HICO image acquired on May 24, 2010. The red mark indicates the former position of the Deep Horizon oil rig

In order to derive diagnostic information on the surface oil, a simple qualitative procedure was used by deriving the spectral response of the oil spill in reference to an uncontaminated surface water spectrum. A spectrum thus obtained includes noise introduced by Fraunhofer lines but represents the general trend in the optical response of the oil spill. Figure 4 shows two examples of spectra that were retrieved within oil contaminated areas. The spectrum in Figure 4a shows that within an oil spill, plant material can be trapped which is indicated by the spectral features that relate to the red edge which is most probably related to the presence of *Sargassum*. Typically, a clean *Sargassum* spectrum resembles the optical behavior of continental plant material and has a strong diagnostic spectral region between 0.692 and 0.710 µm (Gower *et al.*, 2006; Szekielda *et al.*, 2010; Marmorino *et al.*, 2011). However, the low amplitude in the red edge region leads to the conclusion that *Sargassum* covered by oil reduces the probability to recognize it properly.

Strong reflectance in the near infrared was observed over patches of oil which is shown in Figure 4b. At wavelengths below 0.5 µm, absorption is observed and elevated reflectance is observed above 0.55 µm without the presence of major absorption bands. This agrees with observations by Clark *et al.*, (2010a) who found that the color of an oil film taken from the Deep Horizon oil spill on May 7, 2010, has no specific diagnostic absorption bands in the visible. It was also pointed out that the slick's visible spectrum depends strongly on the oil-to-water ratio and entrained air, but only weakly on the emulsion thickness (Clark *et al.*, 2010b).

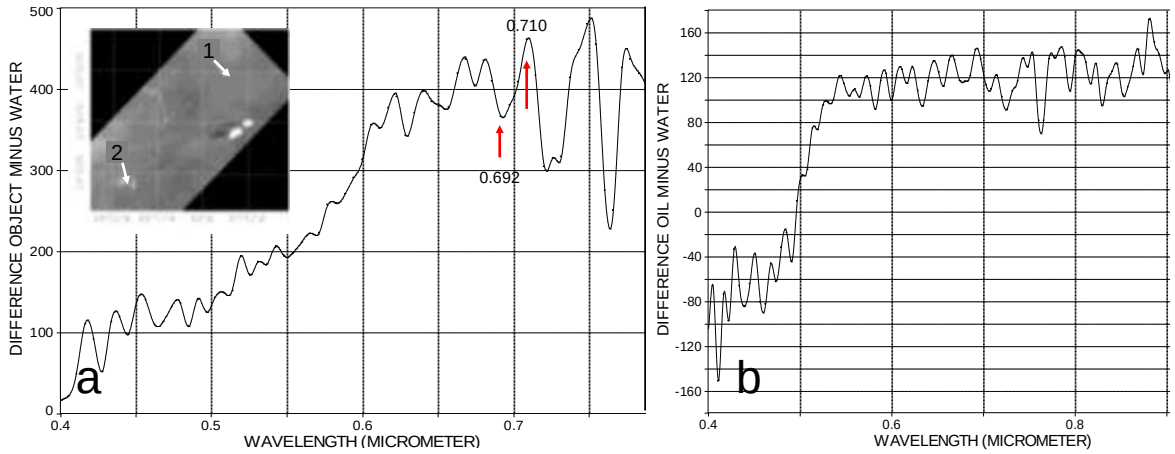

Figure 4: Spectral difference between oil covered surfaces and oil free water as a reference. 4a: Arrows exhibit the spectral range in which *Sargassum* indicates the red edge region. Figure 4b is a spectrum of which the position is given in Figure 5b and was used to recognize oil in the image. The reference clear water spectrum was from the offshore region. Both water spectra were identified as end members with the purity pixel index

The spectral information derived from Figure 4b was applied in generating the RGB shown in Figure 5 taking into consideration the elevated reflectance in the near infrared and the absorption at shorter wavelengths.

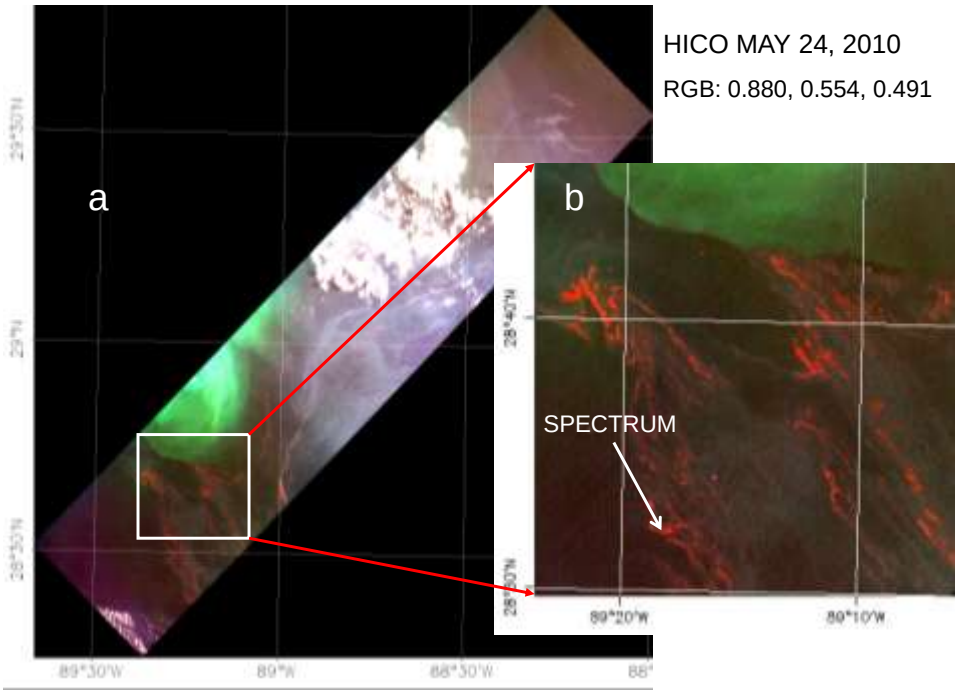

Figure 5: RGB generation with wavebands 0,880, 0.554 and 0.491 µm respectively. The arrow indicates the location where the spectrum shown in Figure 4b was taken

Color composites are very helpful in image interpretation; however, a more refined method for feature separation is through spectral classification which was applied to the HICO image by extracting spectral

end members with the pixel purity index. Processing the data with the end members (see Figure 6) and an algorithm that determines the spectral similarity by calculating the angle between the spectra in the image pixels generates a classified image that is shown in Figure 7. The offshore water is represented as dark blue whereas oil covered areas are displayed in cyan, red and yellow, and the effluent from the Mississippi is displayed in brown.

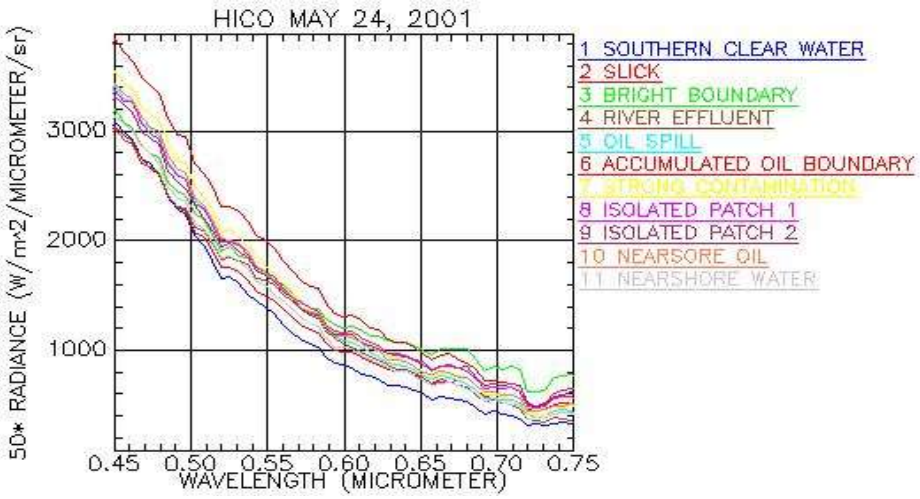

Figure 6: Spectra used for the supervised classification shown in Figure 7b

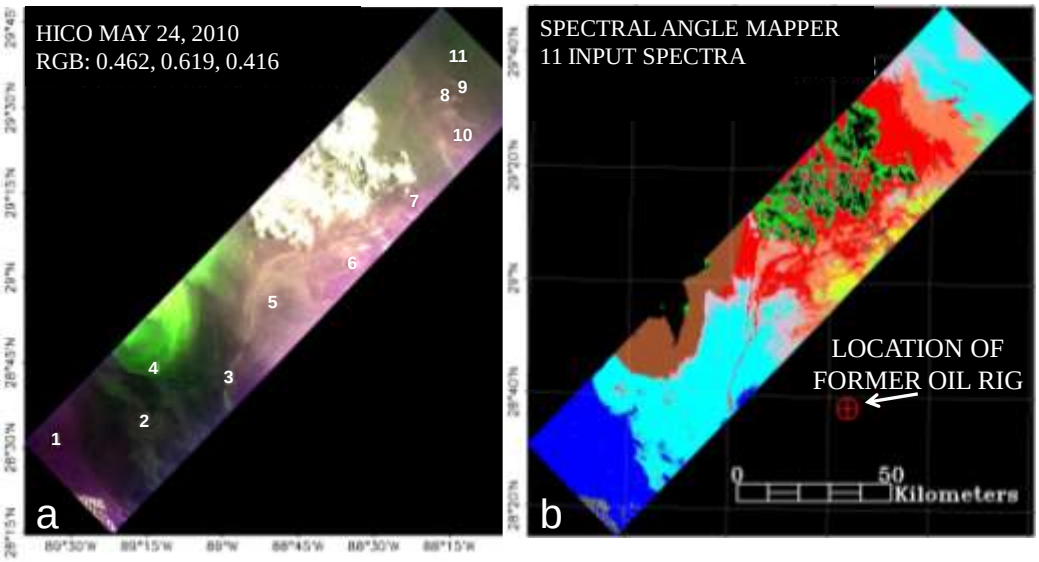

Figure 7a: RGB based on wavelengths 0.462, 0.619 and 0.416 µm with geographical location of spectra that were identified with the pixel purity index and were used as input for the spectral processing (see Figure 6). Figure 7b: Image derived from the input spectra with the location of the former oil rig. Cloud cover is annotated as black and green in the image.

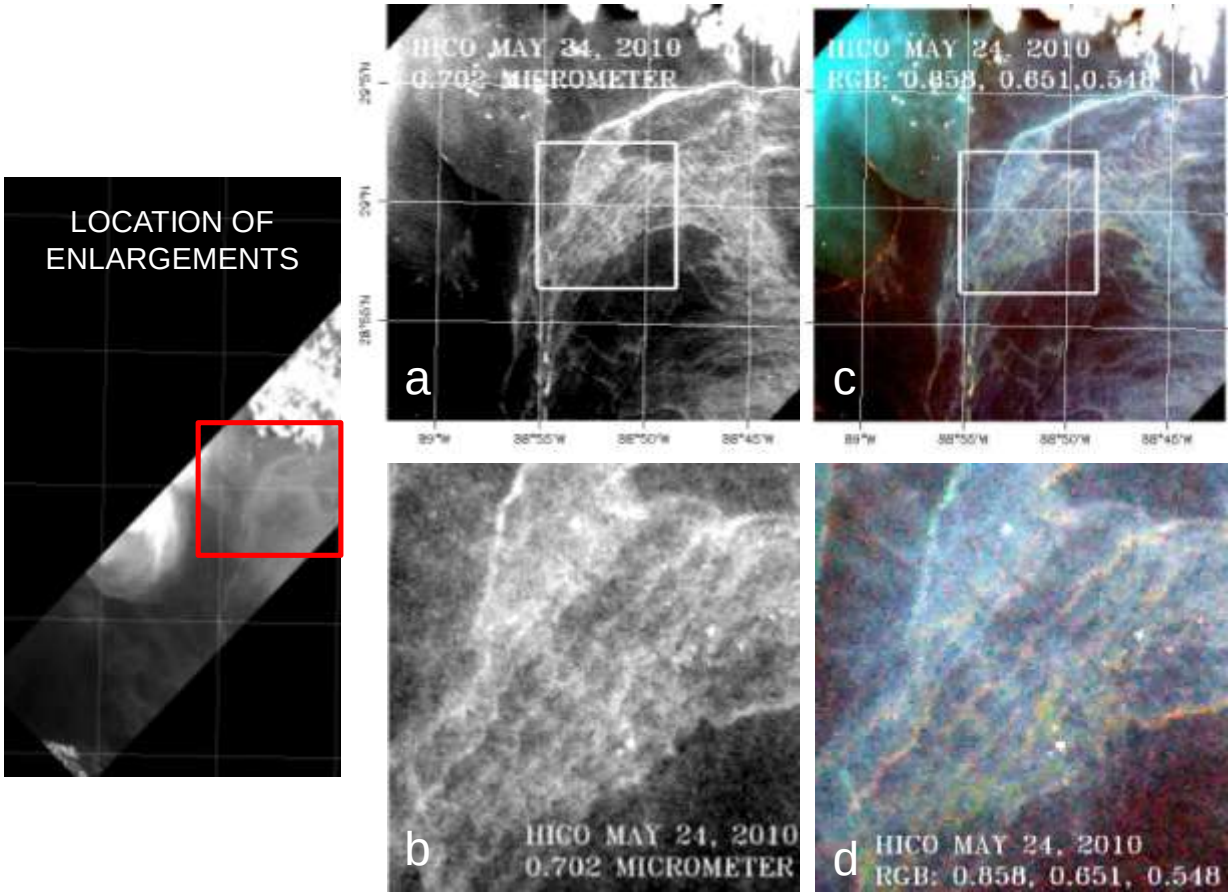

Figure 8: Surface oil distribution in the vicinity of the Mississippi effluent. 8a: HICO image is shown at wavelength 0.702 µm. 8b: Enlarged area of the square in *a*.8c: Color composite (RGB 0.858, 0.651 and 0.548 µm) shows the Mississippi effluent in green and accumulation of oil in streaks. 8d: Enlarged area of the square in *c*.

Streak formation of oil at the surface as identified in Figure 8, seems to be a common mechanism in the spreading of oil and it may be expected that major downward transport of surface oil occurs in those streaks. Earlier satellite studies have shown that internal waves also contribute to accumulation of surface aggregates (Apel *et al.*, 1976) and can be explained by the velocity of surface water that sweeps together surface oils in regions of surface convergence.

At a spatial resolution of HICO data covering 100 m, the spacing of the streaks of around 300 m to 1000 m indicates that internal waves and wind action may be the major cause for the accumulation of surface oil in convergence zones, changing the dispersion of oil from an even surface to an uneven distribution in the form of streaks.

This assumption can be supported by the change in bathymetry near the Mississippi delta that would explain the bending of streaks by refraction of internal waves when approaching the discharge region of the Mississippi.

Such explanation was also provided by Shanks (1987) who showed that some of the surface structures in the distribution of oil spills refer to the action of internal waves and that surface oil can be transported by internal waves through their formation at the shelf break with propagation towards the onshore region through surface currents.

Conclusion

The HICO image revealed the heterogeneity in the distribution of oil and showed that accumulation of some oil appears in streaks that vary in width and length. However, as was cautioned by Leifer *et al.*, (2012), algal material and dark brown oil can appear in a similar alignment, a fact that has also been recognized in our study. This problem has to be addressed when other material aside from oil may accumulate in convergence zones of eddies and current shear. The interpretation of image material has to take further into account the fact that oil accumulation is also generated in convergence zones like Langmuir circulation (Lehr and Simecek-Beatty, 2000) but that this fine-scale is not resolved with HICO. Furthermore, the analyzed HICO image was taken four weeks after the explosion of the rig on 20 April 2010; within that time, a fraction of the spreading oil evaporated, was reworked and weathered, modifying its physical, chemical and spectral appearance. Therefore, it is evident that those changes cannot be extracted from a single image without ground observation and it follows that repeat observations and multi-temporal imaging are required. However, as limited as this study is, it is concluded that hyperspectral observations can be considered as additional inputs in conjunction with other remote sensors for analyzing the dynamics and possible chemical changes of oil spills.

ACKNOWLEDGEMENT

Acknowledgment is given to the support through the NRL/ASEE Summer program.

REFERENCES

Andreoli G, Bulgarelli B, Hosgood B and Tarchi D (2007). Hyperspectral analysis of oil and oil-impacted soils for remote sensing purposes. Office for official publications of the European Communities, *Scientific and Technical Research Series* 34.

Apel JR, Byrne HM, Proni JR, and Sellers R (1976). A Study of Oceanic Internal Waves Using Satellite Imagery and Ship Data. *Remote Sensing of Environment* **5** 125-135.

Brekke C and Solberg AHS (2005). Oil spill detection by satellite remote sensing. *Remote Sensing of Environment* **95** 1–13.

Carnesecchi F, Byfield V, Cipollini P, Corsini G and Diani MM (2008). An optical model for the interpretation of remotely sensed multispectral images of oil spill. *Remote Sensing of the Ocean, Sea Ice, and Large Water Regions*, edited by Bostater CR Jr., Mertikas SP, Neyt X, Velez-Reyes M, *Proceedings of SPIE* **7105** 710501–710504.

Clark RN, Swayze GA, Leifer I, Livo KE, Lundeen S, Eastwood M, Green RO, Kokaly R, Hoefen T, Sarture C, McCubbin I, Roberts D, Steele D, Ryan T, Dominguez R, Pearson N and the Airborne Visible/Infrared Imaging Spectrometer (AVIRIS) Team (2010). A method for qualitative mapping of thick oil spills using imaging spectroscopy *U.S. Geological Survey Open-File Report* 1101.

Clark RN, Swayze GA, Leifer I, Livo KE, Lundeen S, Eastwood M, Green RO, Kokaly R, Hoefen T, Sarture C, McCubbin I, Roberts D, Steele D, Ryan T, Dominguez R, Pearson N and the Airborne Visible/Infrared Imaging Spectrometer (AVIRIS) Team (2010). A method for quantitative mapping of thick oil spills using imaging spectroscopy *U.S., Geological Survey Open-File Report* 1167.

Corson MR, Lucke RL and Davis CO (2010). The Hyperspectral Imager for the Coastal Ocean (HICO) and Environmental Characterization of the Coastal Zone from the International Space Station Conference Paper, Optical Remote Sensing of the Environment, New Sensors and Methods I: Hyperspectral Imaging, Tucson.

Fingas M (1996). The evaporation of oil spills: Prediction of equations using distillation data. *Spill Science & Technology Bulletin* **3** 191–192.

Gower JFR, Hu C, Borstad G and King S (2006). Ocean color satellites show extensive lines of floating Sargassum in the Gulf of Mexico. *IEEE Transactions on Geoscience and Remote Sensing* **44** 3619–3625.

Howari FM (2004). Investigation of Hydrocarbon Pollution in the Vicinity of United Arab Emirates Coasts Using Visible and Near Infrared Remote Sensing Data. *Journal of Coastal Research* **20**(4) 1089-1095.

Jha MN, Levy J and Gao Y (2008). Advances in remote sensing for oil spill disaster management: state-of-the-art sensors technology for oil spill surveillance. *Sensors* **8** 236-255.

Johnson L and Richardson PL (1977). On the wind-induced sinking of Sargassum. *Journal of Experimental Marine Biology and Ecology* **28** 255-267.

Klemas V (2010). Tracking Oil Slicks and Predicting their Trajectories Using Remote Sensors and Models: Case Studies of the Sea Princess and Deepwater Horizon Oil Spills. *Journal of Coastal Research* **26**(5) 789–797.

Le Hénaff M, Kourafalou VH, Paris CB, Helgers J, Aman ZM, Hogan PJ and Srinivasan A (2012). Surface evolution of the deepwater horizon oil spill patch: combined effects of circulation and wind-induced drift. *Environmental Science and Technology* **46**(13)7267-7273.

Lehr WJ, Cekirge HM, Fraga RJ and Belen MS (1984). Empirical studies of the spreading of oil spills. *Oil and Petrochemical Pollution* **2** 7–11.

Leifer I, Lehr WJ, Simecek-Beatty D, Bradley E, Clark R, Dennison P, Hu Y, Matheson S, Jones CE, Holt B, Reif M, Roberts DA, Svejkovsky J, Swayze G and Wozencraft J (2012). State of the art satellite and airborne marine oil spill remote sensing: Application to the BP Deepwater Horizon oil spill. *Remote Sensing of Environment* **124** 185–209.

Liu Y, Weisberg RH, Hu C, Kovach C and Riethmüller R (2011). Evolution of the Loop Current system during the Deepwater Horizon oil spill event as observed with drifters and satellites, in Monitoring and Modeling the Deepwater Horizon Oil Spill: A Record-Breaking Enterprise. *Geophysical Monograph Series*, edited by Liu Y *et al.,* AGU, Washington DC 91–101.

Lucke RL, Corson M, McGlothlin NR, Butcher SD, Wood DL, Korwan DR, Li RR, Snyder WA, Davis CO and Chen DT (2011). Hyperspectral Imager for the Coastal Ocean: instrument description and first images. *Applied Optics* **50**(11)1501-1516.

Lucke RL, Davis CO, Bowles JH, Chen DT, Gao B, Korwan DR, Miller WD and Snyder WA (2010). The Hyperspectral Imager for the Coastal Ocean (HICO™) environmentalittoral imaging from the International Space Station. *Geoscience and Remote Sensing Symposium IGARSS, IEEE Internationa*l 3752 – 3755.

Marmorino GO, Miller WD, Smith GB and Bowles JH (2011). Airborne imagery of a disintegrating *Sargassum* drift line. *Deep-Sea Research* **58** 316–321.

Pugliese Carratelli E, Dentale F and Reale F (2011). On the effects of wave-induced drift and dispersion in the *Deepwater Horizon* oil spill, in Monitoring and Modeling the Deepwater Horizon Oil Spill: A Record-Breaking Enterprise, *Geophysical Monograph Series*, edited by Liu Y *et al.,* AGU, Washington DC 197-204.

Shanks AL (1987). The Onshore Transport of an Oil Spill by Internal Waves. *Science* **235** 1198-1200.

Szekielda KH, Marmorino GO, Bowles JH and Gillis D (2010). High spatial resolution spectrometry of rafting macroalgae (*Sargassum*). *Journal of Applied Remote Sensing* **4** 1-12.

Thiel M and Gutow L (2005). The ecology of rafting in the marine environment I. *The floating substrata, in Oceanography and Marine Biology: An Annual Review*, edited by Gibson RN, Atkinson RJA and Gordon JDM **42** 181–264.